Mingyue Tang
ATMO/OCN 665term-paper
Professor: Kelvin Richards

On How Ocean Mixed Layer Responds to MJO in the Equatorial Indian Ocean: Air-sea Interaction and Turbulent Redistribution

1. Introduction

The Madden-Julian oscillation (MJO) is a subseasonal tropical convective disturbance (Zhang, 2005) and its active phase acts as the storm king in the tropics. Compared with ENSO, MJO nowadays is thought to have the main instability mechanism in the atmosphere rather than in the ocean. However, a recent study also shows that MJO simulations can be improved by coupling oceanic models (Soe, et al., 2008). This suggests the important role of oceanic modulation through both air-sea interaction (Sobel, et al., 2008) and internal ocean processes (Moum, et al., 2016) in various scales, while the ocean's response and feedback to the MJO are poorly known (DeMott, et al.,2015).

Regarded as an eastward propagating large-scale organized tropical convective system, however, large-scale precipitation always accompanies with low SST rather than high SST during active phases of MJO (Benedict and Raindall, 2007), which seems to be inconsistent with the generally positive correlation between large-scale precipitation and underlying surface temperature, while SST variability and SST gradients can still affect tropical atmospheric convection to a great extent (Lindzen and Nigam, 1987). Therefore, MJO research needs to further test the role of small-scale air-sea interaction in such SST feedback, including turbulence redistributing the fluxes of momentum, latent and sensible heat, radiation, and freshwater. Some study even hypothesizes a crucial role of these interactions on the mechanism of MJO initiation (Yoneyama, et al., 2013).

The original purpose of this review study is to answer the question of why the ocean mixed layer appears cooled as low SST during active MJO phases, but I will answer this question with more of a small scale perspective, and extend the question to how the upper ocean mixed layer (ML) are affected from various aspects. To further this point, the air-sea interaction with heat, freshwater, momentum from above by air-sea fluxes and from below by turbulent mixing will be reviewed in section 2, including two papers (Moum et al., 2014; Pujiana et al., 2018) based on the same MJO events from Westerly Wind Bursts observed from a single station point in the equatorial Indian Ocean. Then I will state the opposing opinions and inspired associations in section 3. The last section will list the general conclusions and the take-home points.

2. Responses by Air-Sea Interaction and the Turbulent Redistribution

The MJO events selected here is all between mid-October and mid-December in 2011. At the equator, two positive positive phases of MJO events resulted in a rapid decrease of sea surface temperature (Fig. 1d) , which was also followed by a sustained

period of warming moderated by the cooling effect of ocean turbulence. Our first goal is therefore to explore the physical behind such SST change from the perspective of the air-sea interaction from westerly wind bursts accompanied with positive MJO events.

It has to be noted that all the observation data used here comes from a single spatial point. The research vessel (R/V) Roger Revelle was at 0° , 80.5° E over two cruise legs, on 5 - 28 October and 11 November - 2 December 2011, to measure oceanic and atmospheric processes in connection with studies of the MJO. Primary data sources for this study were meteorological flux measurements (De Szoeke et al. 2015), hull-mounted acoustic Doppler current profiler (ADCP), and Chameleon microstructure profiler. The ocean ML base is denoted by h(t), and the uppermost boundary of the pycnocline is denoted by H(t). The remnant layer is defined as the depth between h and H, acting as the lower layer to affect the upper ML.

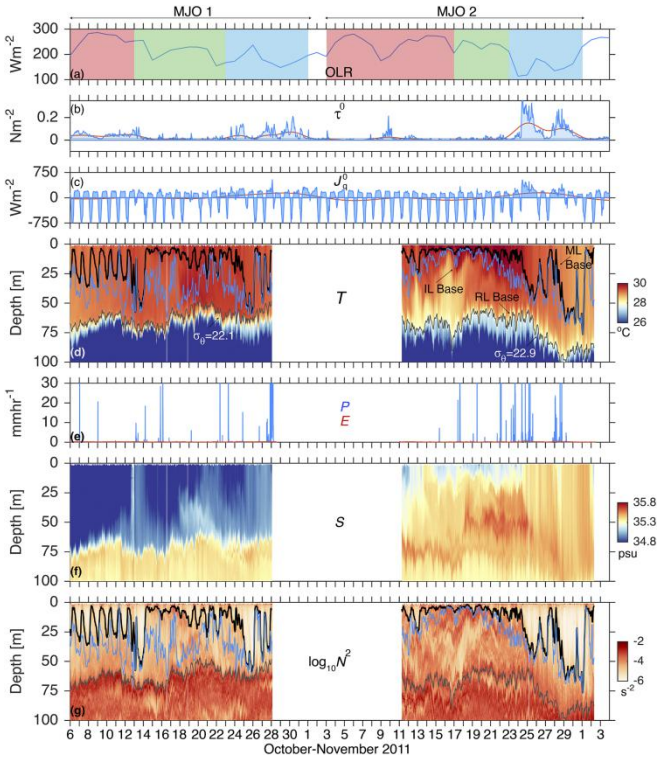

Fig. 1. (Pujiana et al., 2018) Hourly averages of (a) OLR, (b) τ 0, (c) J_q^0 turbulent heat flux , (d) T, (e) P (blue) and E (red) rates, (f) S, and (e) N2 data at 0° , 80.5° E observed over the period of two MJO pulses during 6 Oct – 2 Dec 2011. The data, except the OLR, observed between 6 and 28 Oct and 11 Nov – 2 Dec are from the R/V Revelle, while those observed between 28 Oct and 11 Nov are from the nearby RAMA mooring. For each MJO pulse, shaded areas in (a) mark the suppressed (red), disturbed (green), and active (blue) phases. Thick black contours in (d) and (g) indicate the ML base, while thin gray contours in (d) and (g) represent the RL base. Blue contours in (d) and (g) mark the isothermal layer base.

MJO active phases are defined as reduced OLR here on the equator at 80.5° E (Fig. 1a). Each active phase is associated with one or more westerly wind bursts of

varying magnitude (Fig. 1b and Fig. 2a) followed quickly by an eastward acceleration of the ocean's near-surface zonal current (Fig. 2c). The most obvious heat contribution can be directly seen from the turbulent heat flux at the sea surface (Fig. 1c), for the net surface heat flux changed sign from heating to cooling the sea surface roughly corresponding to the active and suppressed phases of the MJO. However, the contribution of the turbulence that entrains cool water from below is hard to see from Fig. 1, which will be further discussed if we focus more on the active phase.

More detailed observation is shown at only active phase (Fig. 2), where the ML is strongly cooled (Fig. 2d). MJO2 offers a vivid example of the changes brought to the ML by the active phase. The Yoshida-Wyrti jet spinup process were well observed in greater detail in the wake of MJO2 (Fig. 2c), where it accelerated due almost solely to the excess of wind stress over turbulent friction at the base of the jet. Thus, this jet will generate shear turbulence to mix the ML warm water from below, a consequence of the salt-stratified barrier layer.

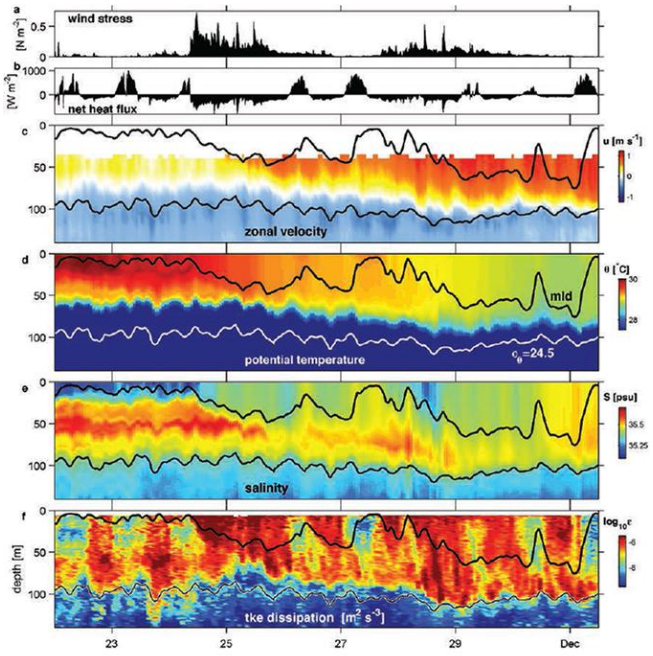

Fig. 2. (Moum et al., 2014) Summary time series of upper-ocean response to the first westerly wind burst of MJO2 at Revelle on 24 Nov 2011. (a) The wind stress (total) appears as a step function change from near-0 to 0.5 N m−2 in a few minutes. (b) Net surface heating. Net surface cooling lasted for more than one day, a rarity at the equator, though common during the passage of MJO events. (c) Zonal current. The eastward surface current (the Yoshida-Wyrtki jet) accelerated from <0.5 m s−1 in about one day, deepening with time. The mixed layer is indicated by the black line, the potential density surface 1024.5 is indicated by the white line. (d) Temperature. Mixed-layer cooling was driven by combined atmospheric and subsurface cooling. (e) Salinity. Salinification of the surface was driven by an excess of subsurface mixing over precipitation. (f) Turbulence dissipation. (bottom) Expanded plots showing the first 24 h following arrival of the wind burst. (g) Wind stress. (h) SST (cool skin correction applied). (i) Temperature with temperature contours scaled to represent identical contribution to density. (j) Salinity, with contours scaled as in (i).

In summary, the mechanisms to cool the ocean ML by the MJO positive events are schematically shown in Fig. 3:

(1) *The cloudiness is widely spread and acts as long lasting stratiform rain during active phases, which significantly reduced the short-wave solar radiation reaching the sea surface as the heat energy input for the ML.*

(2) *Surface heat flux (SW+LW+LH+SH) is reduced by the buoyancy forcing (excess evaporative cooling cooling over solar heating) through the upward turbulent heat fluxes when the surface wind stress is strong.*

(3) *Westerly wind bursts in the lower atmosphere can accelerate the Yoshida-Wyrtki jet because of the shear-induced turbulence and mixing across the thermocline at the jet base. Therefore, the wind stress mixed in the upper ocean generates subsurface mixing to cool the surface ML.*

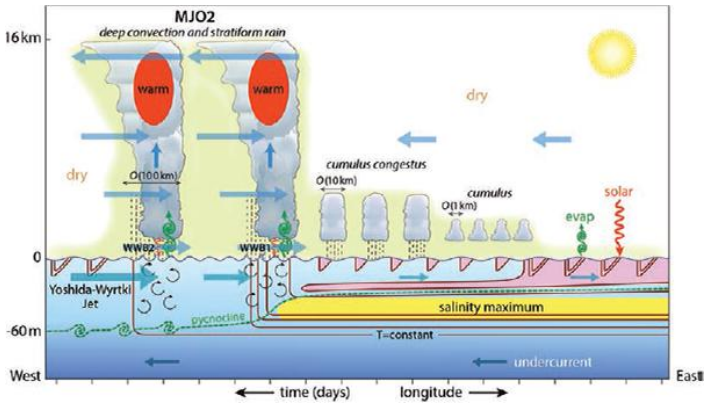

Fig. 3 (Moum et al., 2014) Schematic showing processes observed during MJO2 at 0°, 80.5°E in November 2011. The upper 150 m of the ocean and lower 16 km of the atmosphere are represented as a right-to-left linear time series. This might also be considered a zonal transect along the equator. Green shading in the atmosphere indicates moist air. Pink shading in the ocean indicates the warmest waters, outlined by red isotherms. Near-surface triangles denote diurnal warm layers, with their intensity proportional to the number of isotherms.

The relative contributions of these three mechanisms above are not quantitatively measured and compared in this paper (Moum et al., 2014). However, some later studies argued the third mechanism about that entrainment cooling, albeit indirectly estimated, accounted for a significant cooling in the mixed layer when barrier layers were absent (Hoecker-Martínez et al. 2016); and also deemed that the ML cooled heat budget during active MJOs was primarily driven by surface heat flux and, to a lesser degree, by advection and by other unspecified fluxes (including turbulence) (Chi, et al., 2014), but the data used in this study do not include turbulence measurements. To reply to such arguments and further extend the preliminary mechanisms discusses above, Pujiana and Moum et al. (2018) focus more on the role of subsurface turbulent in governing these responses, which is not adequately represented in model parameterization used in the previous studies.

To firstly estimate the turbulence evolution of the upper-ocean mixing (ML and RL) during all the phases (negative, calm, and positive) of MJO, the turbulent kinetic

energy (TKE) dissipation rate ε and the Richardson number $Ri = N^2 / Sh^2$ will be used here. The ε, which is from the measurement (Moum, et al, 1996) produced by turbulent Reynolds stress τ and turbulent buoyancy flux, representing the dissipation that transforms TKE into heat and has a negative contribution to the local tendency of TKE, is enhanced at specific depths (Fig. 4b) and both of the ML and RL bases (Fig. 4c) during both the calm and active phases. The Ri, whose small value represents more shear-induced turbulence, is significantly reduced at specific depths in ML (Fig. 4d) during the active phases. Thus, the result of the turbulence evolution shows that Sheared currents and consequent strong mixing continued past the active phases, but didn't change significantly during the negative phases.

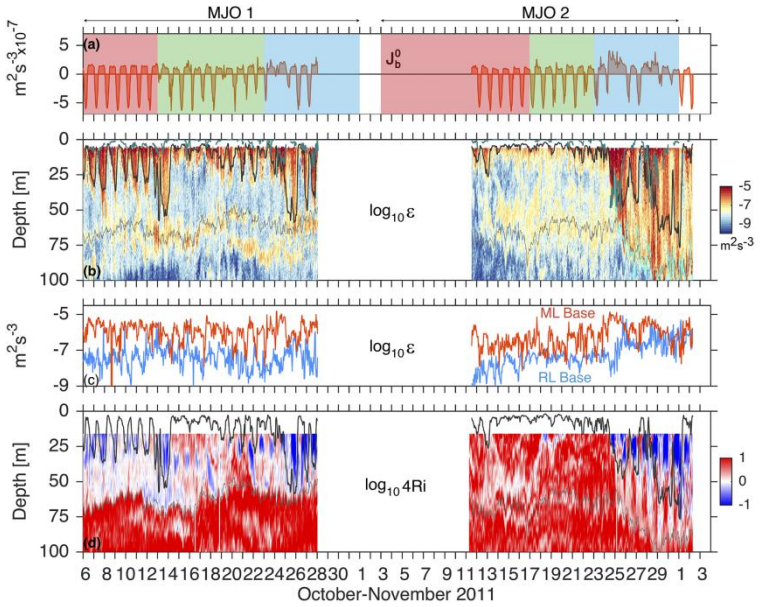

Fig.4. (Pujiana et al., 2018) Hourly averages of (a) , (b) ε , (c) ε averaged over −h − 5 m < z < −h (red) and −H − 5 m < z < −H (blue), and (d) Ri at 0° , 80.5° E during two MJO pulses in 6 Oct – 2 Dec 2011. The ε data are from shipboard Chameleon microstructure profiler. Black, gray, and green contours in (b) and the cyan contour in (b) mark the ML base, the RL base, LMO, and the base of the Yoshida – Wyrtki jet, respectively.

To further estimate the heat, salt/freshwater, and momentum transfers to the ML, the turbulence fluxes are used for budget. The zonal component of the turbulent flux of momentum, or Reynolds stress, is given by

$$\tau_x = -\rho K_m \frac{\partial u}{\partial z}. \quad (1)$$

The turbulent heat J_q and salt J_s fluxes are computed as

$$J_q = -\rho C_p K_T \frac{\partial T}{\partial z}, \text{ and} \quad (2)$$

$$J_s = -K_\rho \frac{\partial S}{\partial z}, \quad (3)$$

where K_m, K_T, and K_ρ are eddy viscosity, turbulent thermal diffusivity, and

turbulent diffusivity, respectively, all of which are estimated basing on the TKE dissipation rate ε. Besides, $\partial u/\partial z$, $\partial T/\partial z$, and $\partial S/\partial z$ are vertical derivatives of zonal current, temperature, and salinity, respectively. Time averaged estimation of these three turbulent fluxes shows their basic vertical distribution. Turbulent heat flux J_q was usually downward ($J_q < 0$) on average, and was substantially intensified during the MJO active phases (not shown here). The turbulent salt flux J_s was generally upward across the upper ocean during all MJO phases, because of to the salinity maximum near the RL base.

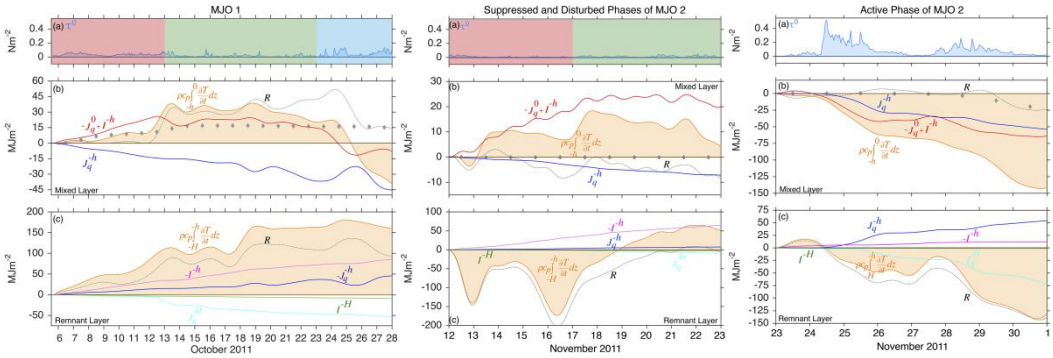

Fig. 5. (Pujiana et al., 2018) The cumulative heat budget in the ML and RL. (a) τ 0. Time-integrated (i.e., accumulated) heating rate and heat fluxes into the (b) ML and (c) RL. Orange curve indicates net heating rate, red curve denotes accumulated surface net heat flux; blue and cyan curves illustrate accumulated turbulent heat flux across the ML and RL bases, respectively; magenta and green curves denote accumulated penetrating radiation at the base of ML and RL, respectively; and dashed line represents residual. A 1.25 cpd low-pass filter is applied to smooth the net heating rate and heat fluxes. Gray diamonds in (b) show time-integrated advective heat flux into the ML inferred from daily averages of shipboard current velocities and spatial gradient of satellite-derived SST. The spatial gradient of SST is computed using centered differences around 0°, 80.5° E using a 0.25° separation.

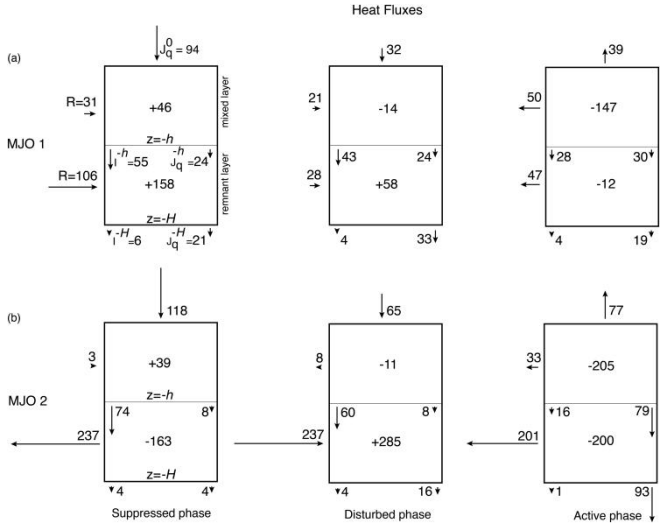

Fig. 6. (Pujiana et al., 2018) Average magnitudes (W m^{-2}) of the cumulative heat budget terms during various phases of (top) MJO 1 and (bottom) MJO 2. The top half of each represents the surface ML, while the bottom half of each represents the RL.

Then the heat transfers mostly by turbulent mixing can be further assessed. The budget of the net ML heating is described by

$$\rho C_p \int_{-h}^{0} \frac{\partial T}{\partial t} dz = -J_q^0 + I^{-h} + J_q^{-h} + R\,, \tag{4}$$

where the fraction of the solar heat flux that penetrates to z = −h, denoted I^{-h}, is estimated from radiation profiles obtained during the experiment (C. Ohlmann 2017, personal communication). The residual R includes unresolved processes (e.g., horizontal advection) as well as observational errors.

For MJO 1, through most of the suppressed phase, the surface ML was warmed by the surface heat flux minus the fraction of the solar flux that penetrated the ML base $-J_q^0 + I^{-h}$ and cooled from below by J_q^{-h} (Fig. 5 left a,b), and the excess of such difference over accounted for 76% of the net heating on average in the ML (Fig. 6a). During the active phase of MJO1, the ML lost heat at an average rate of 147 W m^{-2} (Fig. 5 left a,b, Fig. 6a). The heat loss was partly due to $-J_q^0 + I^{-h}$, with an average cooling rate of 67 W m^{-2}, while the mean J_q^{-h} was -30 W m^{-2} (Fig. 6a). These two dominant factors accounted for 45% and 20% of the net cooling, respectively, and the rest of the cooling was due to the residual. However, MJO2 shows some different features from MJO 1, especially for the residual (advection) term plays relatively a less crucial role through MJO2. During the suppressed phase of MJO 2, the net heating rate in the surface ML was mainly controlled by vertical processes (Figs. 5 middle a,b). In the active phase of MJO 2, the net surface heat flux mostly drew heat from the ocean during two discrete wind bursts (Fig. 5 right a,b). Like $-J_q^0 + I^{-h}$, J_q^{-h} significantly responded to the wind bursts. Turbulence transferred heat across the ML base at an average rate of -79 W m^{-2} (Fig. 6b). The downward continued to cool the ML even after the wind bursts ceased and net surface warming resumed (Fig. 5 right b). However, both of the active phases of MJO 1 and MJO 2 reveal a critical role of subsurface turbulent heat transfer J_q^{-h}, which has the same order of $-J_q^0$ in active phases but much smaller order in negative phases. In other words, only the surface heat flux is the main driver of warming the ML during the negative and calm phases. Nevertheless, both *surface and subsurface turbulent heat fluxes appeared as the main mechanisms playing equally important role in cooling the ML during active phases*.

Similar diagnosis is also applied in studying the salt or freshwater transfers. For the surface ML, the vertically integrated salt equation is expressed as

$$\int_{-h}^{0} \frac{\partial S}{\partial t} dz = J_s^0 + J_s^{-h} + R \tag{5}$$

$$J_s^0 = -S_0\left(P - E\right) \tag{6}$$

where J_s^0 is equivalent surface salt flux, S_0 is surface salinity.

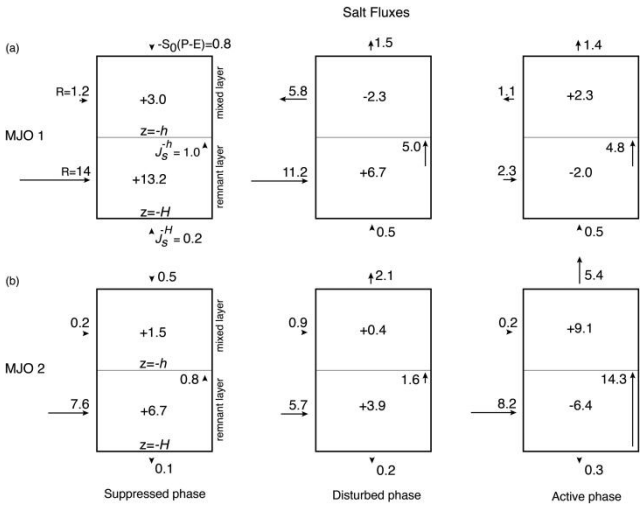

Fig. 7. (Pujiana et al., 2018) Values of the cumulative salt budget terms (psu m^{-1}) during various phases of (top) MJO 1 and (bottom) MJO 2. The top half of each represents the surface ML, while the bottom half of each represents the RL.

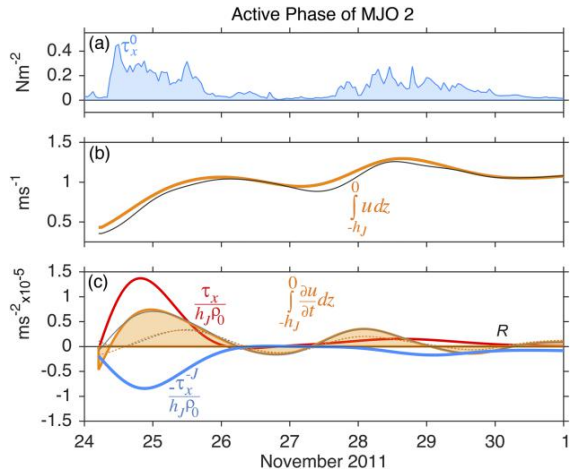

Fig. 8. (Pujiana et al., 2018) (a) . (b) Low-passed u averaged over $-h_J < z < 0$ for uniform u within the upper 12 m (gray) and for linearly extrapolated u within the upper 12 m (orange). (c) Low-passed Reynolds stress at the surface (red) and at $-h_J$ (cyan), zonal acceleration averaged between $-h_J < z < 0$ for uniform u in the upper 12 m (gray) and for linearly extrapolated u in the upper 12 m (orange); $z = -h_J$ is the base of the Yoshida – Wyrtki jet layer. Orange (gray) dashed line indicates residual for the uniform (linearly extrapolated) u in the upper 12-m case. The cutoff frequency of the low-pass filter is 1.25 cycle day^{-1}.

Because active MJO events are regarded as the storm king in the tropics, plenty of precipitation are brought to decrease the surface salt flux to a great extent during the active phases. However, the values of the cumulative salt budget terms (Fig. 7 right) showing increased salt transfers in the ML, which are contrast with previous studies linking the surface salinity response mainly to precipitation and evaporation (Grunseich, et al., 2011; Li, et al., 2015). Especially for MJO 2, The trend of ML salt gain continued during the active phase despite a net freshwater gain of 104.3 mm at

the surface. The total salt input in the ML was 9.1 psu m^{-1}, equivalent to 257 mm of freshwater loss on average, and it was mainly because of the vertical divergence between J_s^0 and J_s^{-h} (Fig. 7 right). These results signify *the importance of subsurface turbulence in governing SSS under MJO convective systems*, and infers the seasonal reason of the monsoon transition-driven eastward current along the equator, which inputs the salt originated from the Arabian Sea and then advected eastward into the RL during the selected months.

The genesis of the Yoshida–Wyrtki jet during the active phase of MJO 2 is the most pronounced dynamic response documented at our station (Fig. 2c), so similar diagnosis of momentum transfers is used to investigate relative contribution of wind stress and subsurface turbulence in accelerating the upper ocean, particularly during the active phase of the MJO. The contribution of subsurface turbulence is assessed through analyses of zonal momentum terms using a conservation equation integrated between the surface and the base of the Yoshida-Wyrtki jet layer $-h_J(t)$:

$$\frac{\partial \overline{u}}{\partial t} = \frac{\tau_x^0}{h_J \rho} - \frac{\tau_x^J}{h_J \rho} + R \tag{7}$$

where $\overline{u}$ is the vertically averaged zonal current, and τ_x is the zonal Reynolds stress.

The zonal current, vertically averaged between the surface and the jet's base, accelerated eastward from about 0.3 m s^{-1} at prewind bursts to 1 – 1.3 m s^{-1} during the wind bursts (Fig. 8a,b). The jet accelerated eastward rapidly following each passage of two wind bursts, while it slowed in the intervening period. *This eastward Yoshida–Wyrtki jet's acceleration is mostly due to the excess of surface wind stress over turbulence stress at the jet's base*, while the residual term cannot be ignored, showing that the surface wind stress was not enough to overcome subsurface turbulence to explain the observed eastward despite its tendency driving 65% of the acceleration.

3. Discussion

Pujiana et al. (2018) demonstrate the importance of oceanic subsurface turbulence mixing, especially its crucial role in vertically redistributing the heat flux to cool the ML in the active phases of MJO, regarded as a response of the dynamical forcing in the atmosphere called WWB. To show the superiority of their methods and data sources, they first criticized some previous articles that used observations and numerical models that included no turbulence and overly shallow modeled ML (Chi, et al., 2014). However, I think there are also some drawbacks to the dataset and methods used in their work, and I would like to suggest some ways in which I think they could be improved or combined for a better understanding of the actual physical processes. First, the biggest problem with this observational data is that it is a vertical sounding of the atmosphere and ocean surface by a ship carrying instruments on a fixed point station in space, 0°, 80.5° E. Though the observing errors caused by ship movement can be better reduced by using Inertial Dissipation than Covariance, a fixed spatial point with a vertical profile cannot reveal its relationship with the

environment around it. Although the advection terms are generally considered to contribute relatively little, the residual term (advection plus errors) is still shown to contribute a lot throughout MJO 1 and during the active phase of MJO 2 (Figs. 5,6), where the advection is even calculated by another dataset from the satellite. A previous study also shows the contribution of heat advection during an MJO event from December 1992 to February 1993 caused by the background temperature gradients, and the roles of such horizontal advection vary with latitudes from 3.5° N to 3.5° S (Kelvin and Inall, 2000). This also infers the restriction of the dataset used by Moum et al. (2014) and Pujiana et al. (2018). The critical role of the subsurface turbulent mixing may not work well at other latitudes and throughout the whole MJO propagation from the Indian Ocean to the Western Pacific, because of the different local limitations of the thermocline depths, MJO center, and the size of convective systems and westerly wind channel in the atmosphere, which are all hard to see from a single station observation.

A short period of abnormalities in the active phase of MJO 1 be related to the problem described above (Fig. 5 left b), where the net ML heating dropped rapidly with a rate about -14 W m^{-2}, but $-J_q^0$ didn't have significant change and J_q^{-h} even increased at about 8 W m^{-2} from 24 October to 26 October 2011, which was not mentioned in this study (Pujiana, et al., 2018). This obvious two-day anomaly may be caused by a heavy precipitation event from my point of view, because the ML can be occasionally warmed the ML following heavy precipitation events, because the rainwater can cool the sea surface and hence reverse $\partial T / \partial z$ (Eq. 2), which consequently led to upward turbulent heat flux warming the surface ML. However, due to the limitation of one single station observation discussed above, we cannot see what actually happened during these two days, whether there was any propagating or just originated atmospheric weather systems could affect the point at 0°, 80.5° E, and how this station point was related to the storm. Why this point is so important in relation to the atmospheric convective systems is largely due to the fact that convective cells are organized in different ways in different regions within the large storm system, which can have very different effects on ocean ML (Thompson, 2016). This study shows that classified by the radar indicated storm type, storms formed in convective systems are more likely to stratify the ocean ML than isolated convective storms based on two reasons. First, although the precipitation system with stratiform rain is usually accompanied by lower number concentration and rain rate, the drop sizes produced by it are much larger thus should be more capable of breaking the surface tension of the ocean to incorporate deeper into the ocean column with which to affect salinity gradients and constitute instability. Second, stratiform can cover a larger area and last longer than an isolated convective cell, therefore more protected freshwater can be produced. In my opinion, this two-day particular period is very much worthy of a more in-depth study, as it likely encompasses more complex sea-air interactions in the case of heavy precipitation during the active phase of MJO. The possible method to improve our understanding about it is to add analysis with real and

idealized cases simulated by the Weather Research and Forecasting (WRF) Model, large-eddy simulation (LES) model, and any coupled air-sea model with high resolution and a process aspect, to certify the storm classification, the spatial relationship, and the internal oceanic processes like Langmuir Circulation.

The problem of selected time scale is also revealed from this ignorance, so I think future work can also separate different time scales in the calculation of changing rate of heat (Fig. 6), salinity (Fig. 7), and momentum, for the averaged rates must filter out some higher frequent waves of important weather effect. Moreover, the facts are obvious that the time scales of MJO, WWB, oceanic Yoshida-Wyrtki jet, and cold pools generated by atmospheric convection are quite different, but the three mechanisms concluded by Moum, et al. (2014) don't consider such timing differences, which means their relative contributions may change throughout the propagation of MJO. Although WWB only covered part of the time during MJO 2, their result shows that after the WWB, turbulence continues to cool the ML even after the surface warming resume, which needs to be further checked for the surprising time lags. A first detailed investigation of the upper ocean response to the strong cold pools associated with MJO was revealed by Pei et al. (2018), where the impact of cold pools was far more significant than WWB during the heavy precipitation. After the period of heavy rain, while net surface cooling remains, SST gradually recovers due to the enhanced entrainment of warmer waters below the mixed layer. They used a one-dimensional ocean model and the situ data collected during DYNAMO located at 1° 30' S, 78° 45' E during the local cold pool event period from 27 October to 28 October 2011, which may be consistent with the special two-day period I mentioned above and can be improved a lot also by using WRF, LES, and coupled air-sea model with high resolution.

The change of ML depth during MJO phases was not discussed by Pujiana et al. (2018), but we can still catch sight of the ML's prominent deepening (mixing) during the active phase of MJO 2 (Fig. 1d). However, what surprises me here is that the ML is also much deeper in the negative phase of MJO 1 than the calm (transition) phase, and the negative phase even reached the same depth as the active phase (Fig. 1d). From my perspective, the difficulty in attributing the evolution of ML depths during different phases of MJO relies on the contrary contribution of ML cooling and freshwater input. During the active phases, stronger Surface heat flux and subsurface turbulent mixing would deepen the ML to a great extent. However, freshwater brought by (stratiform) precipitation could contribute to stratification (shoaling) of the ML by controlling the vertical gradients of seawater density at the same time. This can explain when the remarkable Yoshida-Wyrtki jet and subsurface mixing appeared at the active phase of MJO 2, the first mechanism of cooling would dominate so the ML more significantly deepened, while the active phase of MJO 1 may be affected more by the precipitation refreshing.

Another question about the ML itself is related to the budget method by integrating all the levels (Eq. 4). Though it is always regarded or assumed to be evenly mixed within the ML, I'm a little skeptical that when the Yoshida-Wyrtki jet is present, even though there is more turbulent mixing on either side of it, the oceanic jet

itself might generate a blocking zone like an atmospheric jet, preventing the water on either side of the jet from mixing with each other. In this case, during the active phase of MJO 2, although the subsurface turbulent mixing is super strong, its contribution to cool SST may be less in reality than calculated in this paper.

The last discussion is about the possible ocean's feedback to the atmosphere during MJO propagation. The results here show that the ML and the atmosphere cannot be combined as an isolated system for two reasons. Firstly from the atmospheric perspective, with the clouds changing types and covering area, the input energy by solar radiation and downward longwave radiation by clouds themselves (not discussed) also changes, which can be improved by considering more cloud-radiation feedback. Second, the subsurface mixing is too remarkable to be ignored, which means that the ocean upper layer beneath the ML can also change the surface air-sea interaction from both Ruler and Lagrangian perspectives. Moum et al. (2016) also show the importance of internal ocean process, where the ocean's response to the intense surface winds and cooling by two successive MJO pulses, separated by several weeks, show persistent ocean currents and subsurface mixing after pulse passage, thereby reducing ocean heat energy available for later pulses by an amount significantly greater than via atmospheric surface cooling alone. From a process aspect during the MJO propagating, I can also guess the possible impact by the ocean memory from its subsurface layer, which should produce a more complicated influence on the atmospheric convection. With such ocean internal processes, the question that lower SST but higher SHF during the active phases of MJO would produce larger or smaller energy input to the atmosphere and generate more or less moist patches in the atmospheric boundary layer remains to be a precious inspiration for me.

4. Conclusion

The exact physical process of how the ocean mixed layer (ML) responds to MJO is still an open question. Studies by Moum et al. (2014) and Pujiana et al. (2018) state that both the surface air-sea interaction and subsurface turbulent mixing play crucial roles in redistributing the heat, freshwater, and momentum transfers in ML.

The prominent cooling (warming) ML and SST appear during the active (negative) phases of MJO. During the active phases, The most widely accepted reason is the significant increase in surface evaporative cooling by enhanced turbulent heat flux due to WWB. Moreover, the widespread cloudiness reduced solar radiation reaching the ML. In particular, Pujiana et al. (2018) emphasized the crucial role of turbulence in redistributing the heat flux by subsurface mixing from below, which are equally important as the surface heat flux cooling during the active phases. However, the third mechanism of subsurface mixing is more controversial according to other studies and only works well during active phases.

Though active MJO can bring much more freshwater from precipitation, ML salinity still increases for subsurface turbulence entraining salty advected from ASW by monsoon current, which also causes the asymmetry during active and negative during the selected season. Besides, the generation and acceleration of easterward

Yoshida-Wyrtki jet within the ML during the active phases is mostly due to the excess of surface wind stress as a response to WWB.

Mostly, the ocean ML responds to MJO in such processes above. However, due to the limitation of the observational data and methods used in their papers, future work could help better understand exact physical processes by considering environments, applying numerical models, and separating time scales et al..

5. References

Benedict, J. J., and D. A. Randall, 2007: Observed Characteristics of the MJO Relative to Maximum Rainfall. *J. Atmos. Sci.*, 64, 2332–2354, https://doi.org/10.1175/JAS3968.1.

Chi, N.-H., R.-C.Lien, E. A.D'Asaro, and B. B.Ma, 2014: The surface mixed layer heat budget from mooring observations in the central Indian Ocean during Madden–Julian oscillation events. *J. Geophys. Res. Oceans*, 119, 4638–4652, https://doi.org/10.1002/2014JC010192.

Lindzen, R. and S. Nigam, 1987: On the role of sea surface temperature gradients in forcing low level winds and convergence in the tropics. *J. Atmos. Sci.*, 44, 2418–2436.

Moum, J. N., 1996: Efficiency of mixing in the main thermocline. *J. Geophys. Res.*, 101, 12 057–12 069, https://doi.org/10.1029/96JC00508.

Moum, J. N., and Coauthors, 2014: Air–Sea Interactions from Westerly Wind Bursts During the November 2011 MJO in the Indian Ocean. *Bull. Amer. Meteor. Soc.*, 95, 1185–1199, https://doi.org/10.1175/BAMS-D-12-00225.1.

Moum, J. N., K.Pujiana, R.-C.Lien, and W. D.Smyth, 2016: Ocean feedback to pulses of the Madden–Julian oscillation in the equatorial Indian Ocean. *Nat. Commun.*, 7, 13203, https://doi.org/10.1038/ncomms13203.

Pei, S., T. Shinoda, A. Soloviev, R. Lien, 2018: Upper Ocean Response to the Atmospheric Cold Pools Associated With the Madden-Julian Oscillation, *Geophys. Res. Lett.*, https://doi.org/10.1029/2018GL077825

Pujiana, K., J. N. Moum, and W. D. Smyth, 2018: The Role of Turbulence in Redistributing Upper-Ocean Heat, Freshwater, and Momentum in Response to the MJO in the Equatorial Indian Ocean. *J. Phys. Oceanogr.*, 48, 197–220, https://doi.org/10.1175/JPO-D-17-0146.1.

Richards, K. J., and M. E. Inall, 2000: The upper ocean heat content of the western equatorial Pacific: Processes controlling its change during the Tropical Ocean - Global Atmosphere Coupled Ocean-Atmosphere Response Experiment. *J. Geophys. Res.*, https://doi.org/10.1029/2000JC900012.

Seo, H., A. C.Subramanian, A. J.Miller, and N. R.Cavanaugh, 2014: Coupled impacts of the diurnal cycle of sea surface temperature on the Madden–Julian oscillation. *J. Climate*, 27, 8422–8443, https://doi.org/10.1175/JCLI-D-14-00141.1.

Sobel, A., E.Maloney, G.Bellon, and D.Frierson, 2008: The role of surface heat fluxes in tropical intraseasonal oscillations. Nat. Geosci., 1, 653–657, https://doi.org/10.1038/ngeo312.

Thompson, E. J., 2016: Tropical warm pool rainfall variability and impact on upper

ocean variability throughout the Madden-Julian oscillation. Ph.D. thesis, Colorado State University, 217 pp.

Yoneyama, K., C.Zhang, and C. N.Long, 2013: Tracking pulses of the Madden–Julian oscillation. *Bull. Amer. Meteor. Soc.*, 94, 1871–1891, https://doi.org/10.1175/BAMS-D-12-00157.1.

Zhang, C., 2005: Madden-Julian oscillation. *Rev. Geophys.*, 43, RG2003, doi:10.1029/2004RG000158.